THE UNIVERSITY OF MICHIGAN

INDUSTRY PROGRAM OF THE COLLEGE OF ENGINEERING

A TARGET SIMULATOR FOR CONICAL SCAN RADARS

Lyman W. Orr

December, 1957

IP-255

ACKNOWLEDGEMENTS

ABSTRACT

A target simulator for conical scan radars is described which permits study of the dynamic response of the radar to typical targets within a laboratory environment. A predetermined trajectory is generated by mechanical cams giving the variations of azimuth, elevation and slant range of the simulated target. These quantities are electrically compared by means of synchros to the corresponding quantities in the radar, and result in the generation of error signals. The azimuth and elevation errors are combined, and converted to a suitable modulation wave by an optical device which takes into account the antenna lobe shape. This wave modulates a train of pulses at the IF frequency of the radar, which after suitable attenuation is fed to the radar IF input. Provision is made for introducing interference signals along with the pulse train for jamming susceptibility studies.

The simulator was designed to operate with the AN/MPQ-10A mortar-tracking radar, but can readily be adapted to other conical scan radars.

A TARGET SIMULATOR FOR CONICAL SCAN RADARS

I. INTRODUCTION

The Electronic Defense Group at The University of Michigan is concerned with susceptibility of mortar-tracking radars to various types of jamming signals. To avoid the high cost, inconvenience and time consumed in field testing, some means of testing the radar within a laboratory environment was needed.

This need led to the development of a target simulator for conical scan radars, such as the AN/MPQ-10A mortar tracker. When used in conjunction with the simulator, the radar tracks the simulated target and exhibits the same dynamic response as it does under field conditions with a real target. Therefore extensive laboratory investigation of the dynamic response of the radar to typical mortar trajectories is now possible under a variety of test conditions.

II. TYPICAL TARGET

A typical target to be simulated is an 81 mm mortar shell fired with a muzzle velocity of 700 feet per second at an angle of 63 degrees from the horizontal, as indicated in Figure 1. For flat terrain, this gives a missile range of 4,000 yards and a flight time of 39 seconds. The path of the simulated target is predetermined by a set of three mechanical cams. These cams are precision machined from computed values, and establish the azimuth, elevation and slant range of the target at any instant of flight.

1

III. MODULATION DUE TO CONICAL SCANNING

In a conical scan radar, the radar antenna beam or lobe spins about the radar tracking axis describing a circular cone. Figure 2 is a space view as seen from the radar. It shows the motion of the lobe axis B about the radar axis RA. A target T, located in the field induces a response in the radar, and this response or echo is modulated by the changing angle BT during scanning because of the lobe shape. The pointing error is the angle Θ between the target T and the radar axis RA. Its vector components Θ_a and Θ_e are the azimuth and elevation errors. If the pointing error is reduced to zero, the target is on the radar axis RA, and no modulation of the echo results because the angle BT would then remain constant during scanning.

In the MPQ-10A radar, the conical angle between the radar axis and lobe axis is 1.5°, the half-power beam width is 5° and the scan rate is 60 cycles per second. The shape of the lobe is assumed to be a figure of revolution with an electric-field-fall-off law of $(\sin x)/x$. Since there is a similar fall-off for the received echo signal, the antenna voltage response, V_r has the form

$$V_r = (K \sin^2 x)/x^2 \tag{1}$$

where K is a constant determined by the range, target cross section and peak pulse power, and x is proportional to the angle α between the target and the instantaneous position of the lobe axis.

As the pointing error Θ assumes various values, the echo signal is modulated as indicated in Figure 3. It is seen that for values between 0° and 1°, the modulation increases with Θ and is approximately sinusoidal. For larger errors, the modulation departs noticeably from sine form, and increases to a maximum at $\Theta = 2.5°$. As the error increases above 2.5°, the

modulation and signal strength both decrease, becoming negligible at about $7°$. The relative phase of this modulation is determined by the relative sizes of θ_a and θ_e. All these effects must be taken into account in designing the simulator.

Azimuth and elevation errors are sensed in the radar by means of two phase-sensing detectors which use for comparison two 60-cycle reference voltages which are in time quadrature. In the field, these voltages are furnished in the radar by the spinner generator attached to the beam spinner. In the simulator, the azimuth and elevation reference voltages are furnished by an external source operating from the 60-cycle line. This change is required because in operating the radar with the simulator, the microwave circuits and beam spinner are inoperative.

IV. SIMULATOR OPERATION

Overall operation of the simulator may be understood by referring to Figure 4. This block diagram shows that the system is a closed loop servo, with provision for introducing interfering signals at one point in the loop, namely at the input to the radar IF amplifier. The complete radar set and radar control panel are indicated by the two blocks on the lower right. The only changes from field operation are that the microwave circuits and beam spinner are rendered inoperative, and that two control transmitters have been attached to the antenna turret. All other blocks are contained in the simulator rack, and connected to the radar by means of flexible cables which permit the normal motions of the turret.

The reference generator is indicated just above the control transmitters. Using 3-phase line power, it produces two 60-cycle voltages in quadrature, namely

the azimuth and elevation reference voltages. These are coupled to the phase-sensing detectors in the radar, and also to the rotors of the azimuth and elevation synchro control transmitters. These rotors are mechanically coupled to the radar mount so that their rotor positions correspond to the azimuth and elevation of the mount.

The stators of these control transmitters (CX) are electrically connected to the stators of corresponding control transformers (CT). If the rotors of the CT's are oriented at 90° from their corresponding CX's, as indicated diagrammatically in Figure 4, both CT outputs will be zero.

The positions of the CT rotors are controlled by the azimuth and elevation cams, and as the cam carriage moves, information regarding the position of the target in relation to the radar is sensed by the CT outputs. For an error in azimuth, the output of the azimuth CT will be a 60-cycle sine voltage whose magnitude is linearly proportional to the azimuth error, while the phase will be the same as or 180° from that of the azimuth reference voltage, depending on the sign of the error.

The outputs of the azimuth and elevation CT's are added in a 60-cycle adder. For an error in both azimuth and elevation, these voltages, being in quadrature, produce at the adder output a vector sum whose magnitude and phase angle correspond to the magnitude and space orientation of the pointing error.

Before being used to modulate a train of pulses, the 60-cycle adder output must be treated so that modulating functions corresponding to Figure 3 will be generated. This operation is performed by the Antenna Beam Shape Generator. This unit, discussed below in more detail, consists of an oscilloscope, a phototube, and appropriate shaping circuits. In addition to producing the correct lobe shape, or modulating function, the phase information from the

4

60-cycle adder is retained. Correct separation of the azimuth and elevation errors can thus be accomplished by the radar in the normal manner.

The output of the Beam Shape Generator is amplified and fed to the modulator unit. This consists of a 30 MC IF amplifier having an external AGC connection. Because the gain of the IF amplifier is a non-linear function of the AGC voltage, it is necessary to use a function generator ahead of the AGC input. The function generator circuit is shown in Figure 5, and consists of biassed diodes and resistors. It is designed to have a transfer function which is the inverse of the AGC-gain characteristic. Thus the combination of function generator and IF amplifier produces a linear modulator.

The RF input to the modulator is a train of pulses of 30 MC energy produced by a keyed oscillator. Each pulse has a duration of 0.8 microsecond, and the repetition rate is 1120 pps. The beginning of each pulse is delayed from the radar's sync or trigger pulse. The delay is variable, and is determined by the position of the range cam which operates a potentiometer in a phantastron delay circuit. As the range of the simulated target varies, it is tracked by the range gate in the radar.

From the above it may be seen that the modulator output is a train of 30 MC pulses having envelope modulation according to Figure 3, and carrying pointing error and range information. This pulse train is suitably attenuated and fed to the input of the radar IF amplifier. Prior to attenuation, an RF power meter determines the power level. By using the radar equation and the known parameters (target cross section and range, peak microwave power, beam width, and crystal mixer loss), the proper attenuator setting is calculated for the situation to be simulated.

At this point in the circuit, provision is made for the introduction of
interfering signals with adjustable attenuation. This is indicated in Figure
4 by the noise source and right-hand attenuator. Performance studies can thus
be made under a variety of test conditions.

V. TRAJECTORY CAMS

Precision cams are used to generate the trajectory of the simulated target.
The cam assembly and linkage for the elevation channel is shown in Figure 6.
The cam carriage rolls on precision ball bearings along a carefully machined
pair of rails. A constant speed carriage motor drives the carriage in either
direction at 0.1 inch per second. In a typical 39 second trajectory, the car-
raige thus moves a distance of 3.9 inches. Reversing limit stops give automatic
carriage motion reverse. A manual reverse is also furnished for convenience.
Figure 7 shows the carriage cams and followers. The central range cam was not
installed when this photo was taken.

The cams are machined from 1/16 inch steel gage stock. The trajectory is
calculated for each second of flight, and the azimuth, elevation and slant range
computed. From these three sets of data five-times scale drawings of the three
cams are made. By accurate photoreduction, the contours are photoengraved[1]
directly on the steel cam blanks. The photoengraved lines are 5 mils wide, and
result in a machining tolerance of ± 2.5 mils. The machining tolerance leads
to a parameter tolerance of ± 0.25° in azimuth and elevation and ± 25 yards
in slant range.

Several sets of cams were produced for different trajectories and different
aspect angles (missle path relative to radar position). A quick change feature
is incorporated which allows the set of three cams to be changed in a few

---

[1]A. Rock and J. Cooper "Precision Photoengraving of Machine Parts," Industrial
Photography,v.6, No. 11, (to be pub. Nov. 1957).

seconds, thus no set-up time is needed in changing trajectories.

The mechanism illustrated in Figures 6 and 7 transfers the cam follower motion to the control transformer. The elevation position potentiometer shown in Figure 6 is also driven by the mechanism, and is used for monitoring. A typewriter carriage-return spring maintains tension on the instrument chain, and takes up any slack in the mechanical linkages.

Figure 8 shows the connections to the elevation control transmitter (CX) and control transformer (CT). The output of the CT is a 60-cycle sine voltage proportional to the elevation error. Figure 9 shows the corresponding connections for the azimuth channel. In this case a cosine transformer was needed ahead of the CT rotor winding. This was necessary to account for the fact that the angular space error when the radar is in an elevated position, is less than the actual azimuth error by the cosine of the elevation angle E. The cosine transformer is coupled to the elevation gearbox to produce maximum output for E = 0°. At other elevation angles, the size of the azimuth error is suitably reduced by cosine E.

As noted previously, the azimuth and elevation error signals are added together to produce a combined error signal. This is done by the network shown in Figure 10 consisting of two 10 K input resistors in series with a common 1 K output resistor. The 60-cycle error signal at the output resistor is proportional to the vector sum of the two input signals, and is fed to the Antenna Beam Shape Generator.

VI. ANTENNA BEAM SHAPE GENERATOR

We now come to the most difficult task in the design of the simulator. This is the conversion of the 60-cycle error signal from the adder to a suitable modulation wave which takes into account the shape of the antenna lobe (Equation 1), and retains the phase of the error signal.

The first part of this task consists in the design of a conversion device which will simulate the lobe shape in two dimensions. Several schemes were considered, but the one finally adopted makes a compromise between precision on the one hand, and simplicity and reasonable cost on the other. This scheme uses a cathode ray tube with uniform phosophor response over the face of the tube. The tube has a flat face and type P 11 phosphor. It is driven by conventional oscilloscope circuitry except that the deflection amplifiers and high-voltage power supply must be particularly free of hum and ripple. A vacuum phototube is mounted as shown in Figure 11 at a distance d from the cathode ray screen. Because of its small circular aperture and S9 response, a type 1P42 phototube is used.

To describe the optical performance, a luminous cathode ray spot of constant diameter and brightness is assumed. When this spot is displaced a radial distance x from the phototube axis, the light flux L_p entering the phototube is governed once by the inverse square law and twice by the cosine law. Thus it may be expressed as

$$L_p = (k \cos^2 \emptyset)/r^2 \tag{2}$$

where k is a constant, $\cos \emptyset = d/r$ and $r^2 = x^2 + d^2$. After substitution, this can be reduced to the simple form

$$L_p = L_o [(x/d)^2 + 1]^{-2} \tag{3}$$

where L_o is the light flux entering the phototube for x = 0.

The relative phototube response is linear with light flux, so that its variation with x is also expressed by Equation 3, and this is plotted in Figure 11a. A brief inspection of this curve indicates that it is a very poor fit to the desired antenna lobe shape given by Equation 1. However, if one chooses a new reference level at the 25% response point, as indicated in Figure 11a by the dashed horizontal line, the portion of the response curve above this line can be closely matched to the desired curve. The theoretical match is shown in Figure 12, when the horizontal scale of the phototube curve is adjusted to match the antenna lobe pattern at the match point (0.5 response at 2.5°). Thus the combination of CR tube, phototube and reference level circuit produces the desired results.

The second part of the task is to cause the luminous spot to move over the phosphor screen in such a way that its radial distance from the phototube axis (the distance x) corresponds to the instantaneous angle α between the target and lobe axis. This is accomplished in two operations.

Operation one. The error signal is converted to a circular spot motion by coupling it to the X and Y amplifiers of the oscilloscope, but delaying the Y signal by 90° in the 90° phase shift network indicated in Figure 4. By making appropriate gain adjustments, the circular trace is obtained. An increase in the size of the error signal causes a proportionate increase in the diameter of the circular trace.

Operation two. The phototube axis is displaced in the positive X direction a distance corresponding to 1.5° from the center of the circular trace. By simple geometry it can be shown for any given angle of pointing error θ, that the varying distance x between the spot and the phototube axis corresponds exactly to the varying angle α between the target and the radar lobe during conical scanning.

The preservation of phase in the phototube output may be shown by considering the situation with only a positive azimuth error. In this case the error signal fed to the oscilloscope is in phase with the azimuth reference voltage. Since the circular spot motion is produced by an in-phase signal to the X amplifier, the spot will be closest to the phototube axis at the time the input signal reaches its maximum. Since the phototube response is a maximum here, phase is preserved in the phototube output.

The phototube and reference level circuit is shown in Figure 13. The 1P42 phototube has a 50 megohm cathode load and cathode follower. The choice of the cathode follower tube is made to minimize grid current, and the left portion of the 12AV7 is operated at a grid-to-cathode voltage for zero grid current to insure linear loading of the phototube.

With no light entering the phototube, the output of the cathode follower (left half of the 12AV7) is below the voltage at point A, and crystal diode XL501 does not conduct. In this case XL502 conducts, and the voltage at point A (the output voltage) is established by the setting of the reference level control, R505. As increased light enters the phototube, the cathode follower output eventually exceeds the quiescent voltage at A. In this case XL502 conducts and XL501 is non-conducting. Thus, as the light flux rises above the reference level, the output voltage increases in proportion. A third diode, XL503, acts as a clamp preventing a negative output voltage during warmup.

The reference level is nominally set at 25% of the maximum phototube output for the best curve match. In practice, the level is set with the aid of a monitor scope. The spot is driven horizontally at 60 cycles and the output waveform is observed against a $\sin^2 x / x^2$ plexiglass overlay on the monitor scope. The reference level, and horizontal and vertical gains are adjusted

10

for the best fit.

After completing the adjustments, the input circuits are restored to normal, and the output of the reference level circuit now gives the required modulation wave (as in Figure 3) for any error signal. This modulation wave is amplified in a DC amplifier, and fed to the modulator which was discussed above.

VII. PULSE GENERATOR AND OSCILLATOR

The RF input to the modulator is generated as indicated in Figure 14. A synchronizing pulse from the radar is used to trigger a phantastron delay circuit. The amount of delay is determined by the range cam which operates a low torque potentiometer in the phantastron timing circuit. A typical target range of say 5000 yards is correctly represented by a delay of 30.5 microseconds. The trailing edge of the phantastron output (Figure 14c) triggers a one-shot multivibrator which produces the 0.8 microsecond gate pulse (Figure 14d). This gates on a ringing oscillator for the duration of the gate, and produces a series of pulses of 30 MC energy (Figure 14e). An output cathode follower is added to drive the 50-ohm coaxial output cable.

A general view of the simulator is shown in Figure 15. The monitor scope is at the top left, while the beam shape generator and phototube amplifier is at the top right. Below these are found the two precision attenuators and the cam carriage assembly. Following these are the meter switching panel, RF power meter, reference level voltmeter, and, at the bottom, the 60-cycle azimuth and elevation reference voltage generator.

VIII. SUMMARY

The Michigan Radar Target Simulator generates, in a laboratory environment, a variety of mortar shell trajectories which induce in the radar a dynamic response similar to that obtained in the field with a real target. The trajectory of the simulated target can be quickly changed by installing a new set of cams. Although designed to match the scan rate, beam shape and conical scanning angle of the MPQ-10-A mortar tracker, other types of radars may be tested by making relatively simple changes in the simulator. Radar behavior studies such as jamming susceptibility are being conducted here with a high degree of success.

TRAJECTORY

$h = r/2$

ϕ FIRING ANGLE

MORTAR

BURST POINT

r
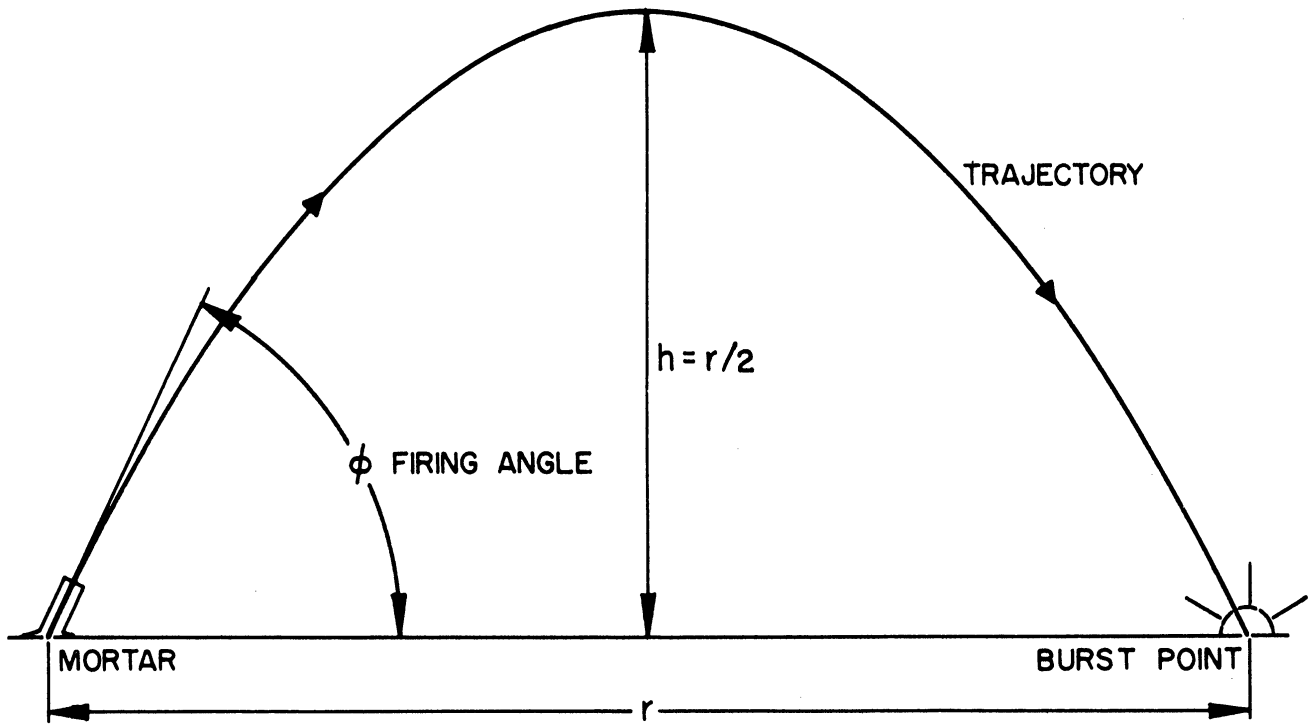
Figure 1 Elevation View of Typical Trajectory
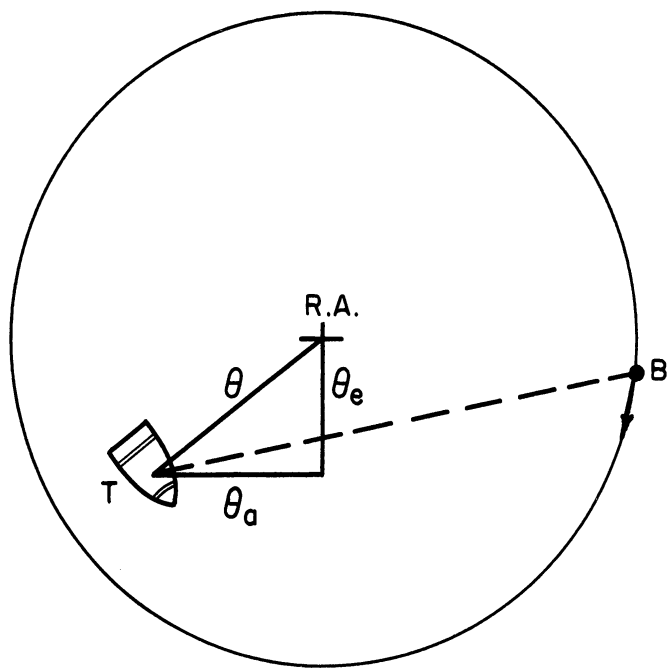
Figure 2 Radar View of Target
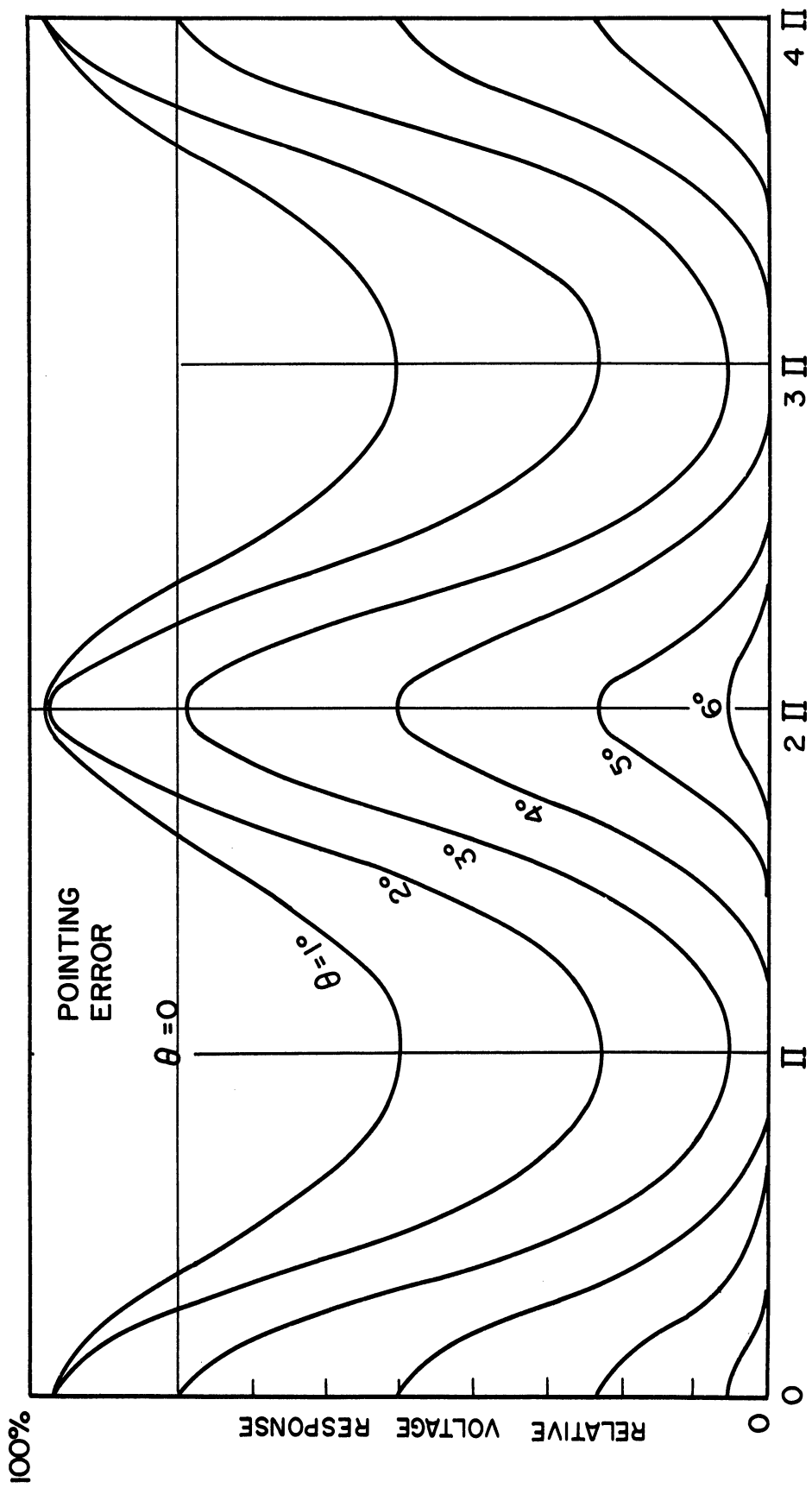
Figure 3   Modulation of Echo Signal
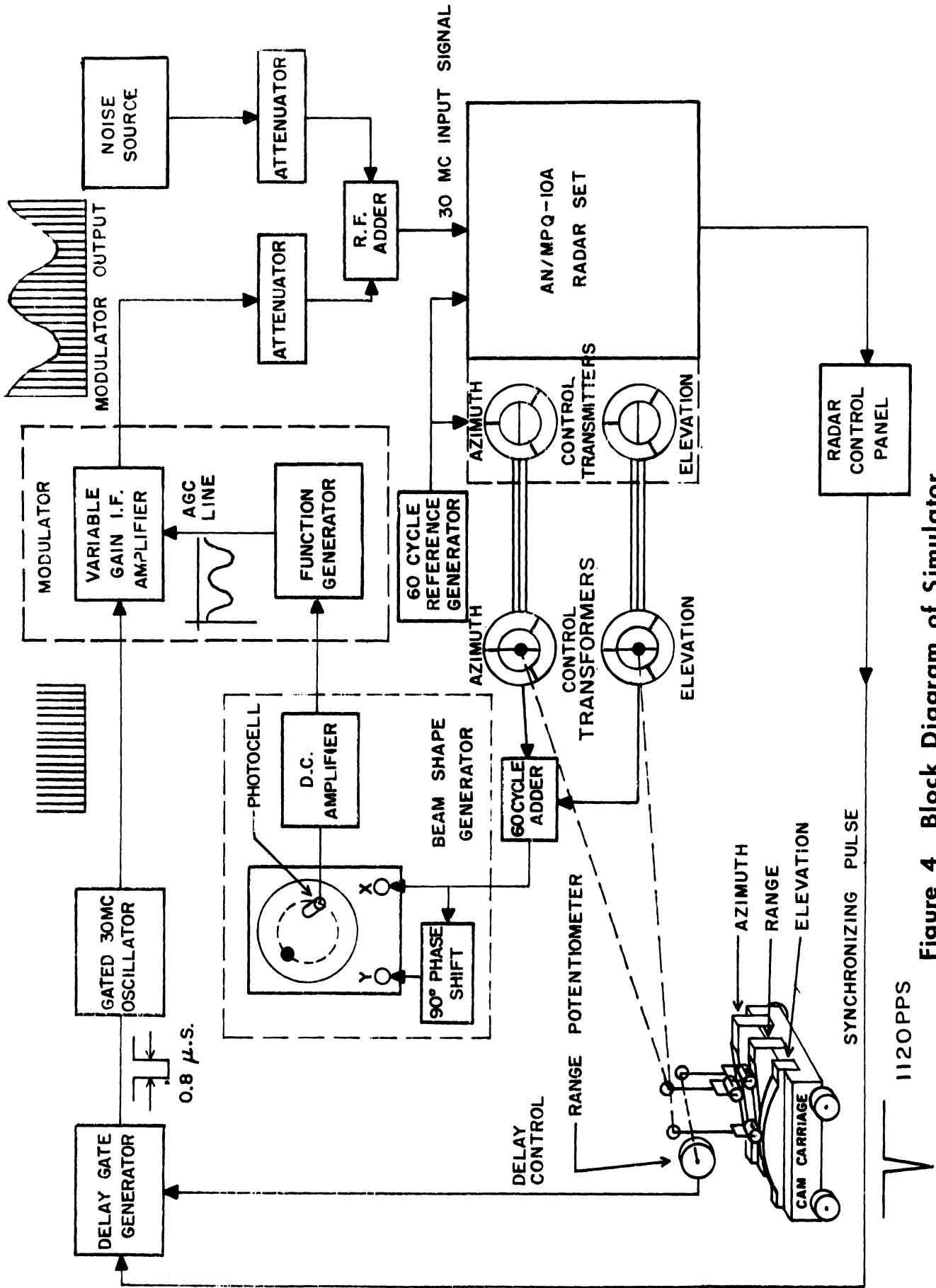
Figure 4 Block Diagram of Simulator

R4I0

R4II   R4I2

INPUT VOLTAGE   OUTPUT VOLTAGE

FROM DC   CR4OI   CR4O2   TO I.F. AMPLIFIER

AMPLIFIER V_1 V_2 IN MODULATOR

$$|V_1| < |V_2|$$
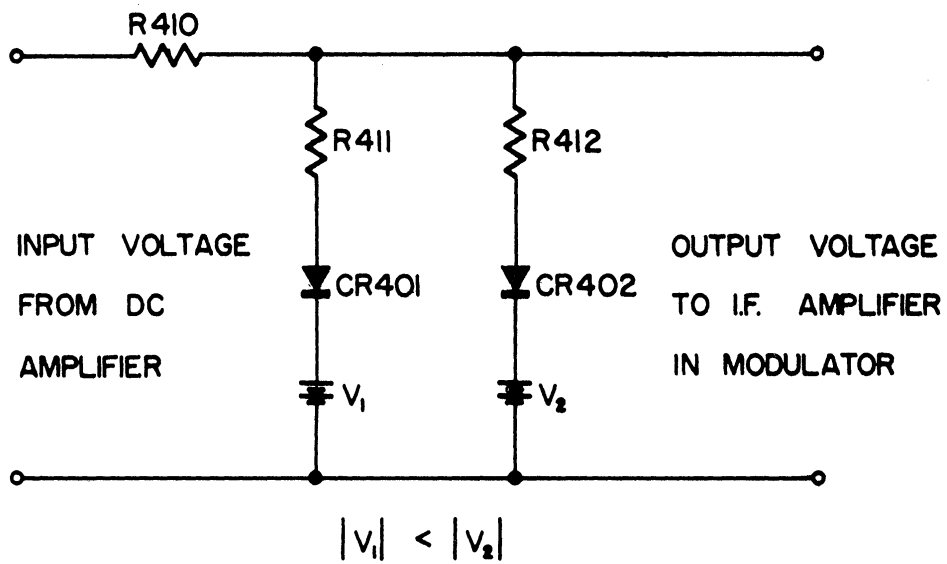
Figure 5   Function Generator Circuit
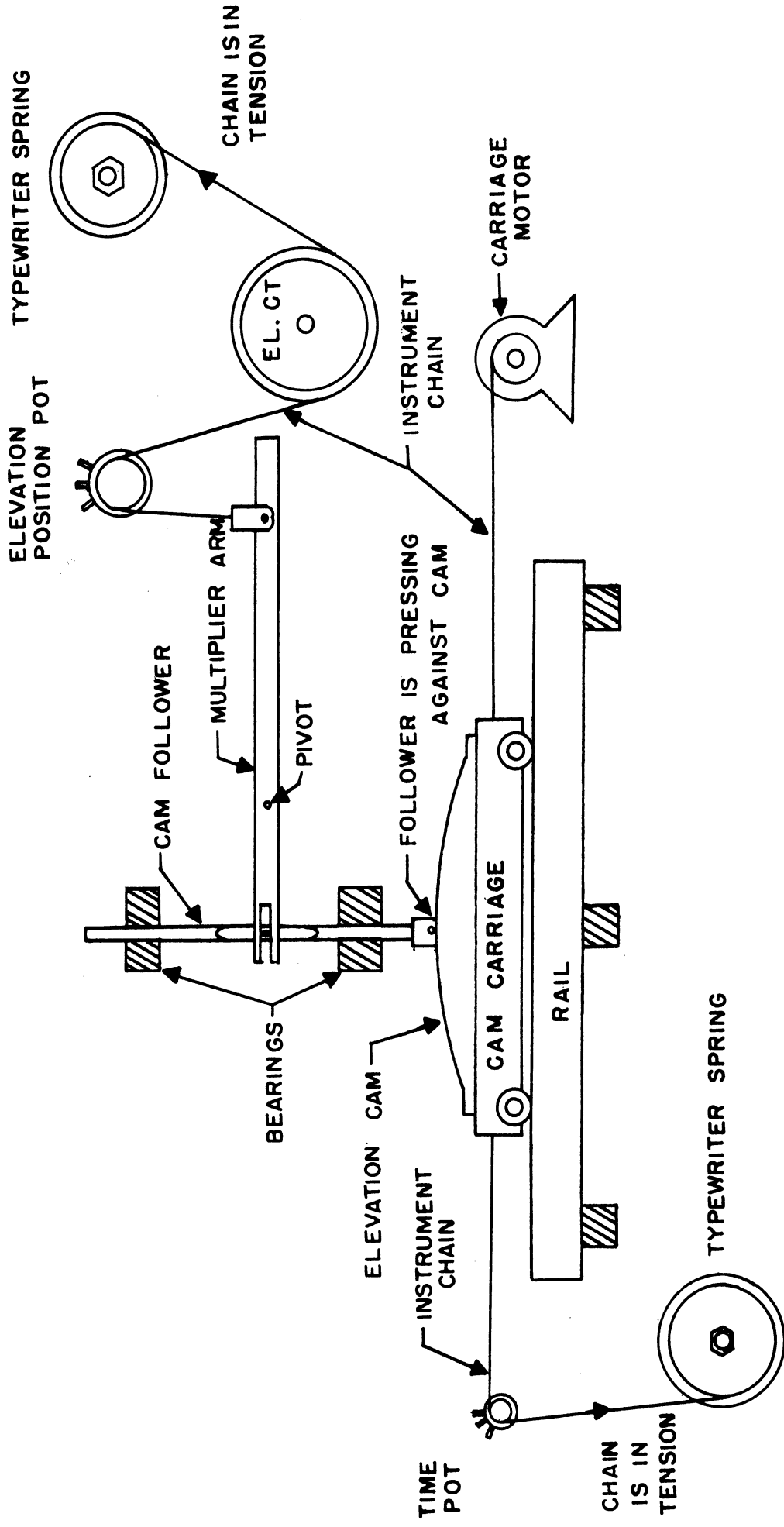
Figure 6   Cam Linkage for Elevation Channel
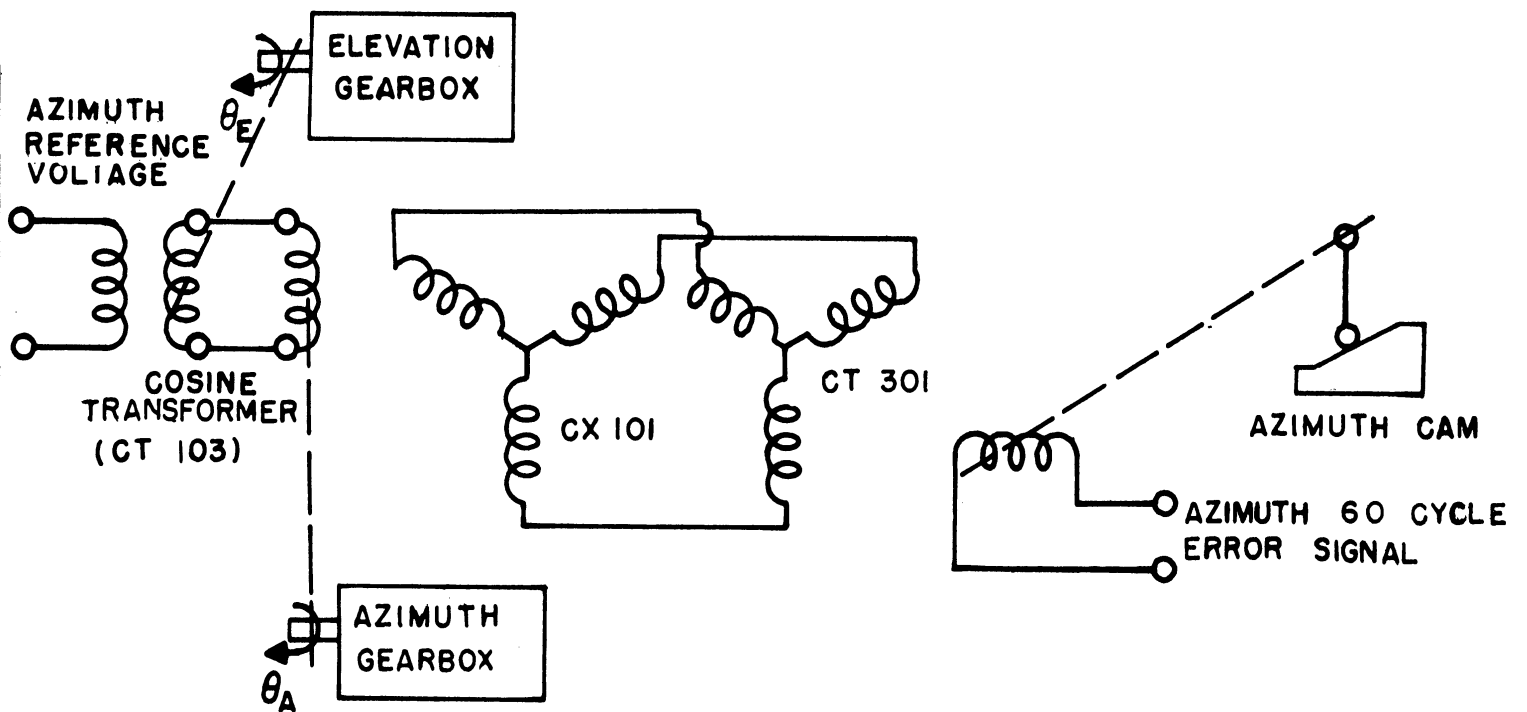
Figure 7   Cam Carriage Assembly

ELEVATION
REFERENCE
VOLTAGE

ELEVATION
CAM

CX 102

CT 302

ELEVATION
GEARBOX

θ_E

ELEVATION
60 CYCLE ERROR
SIGNAL
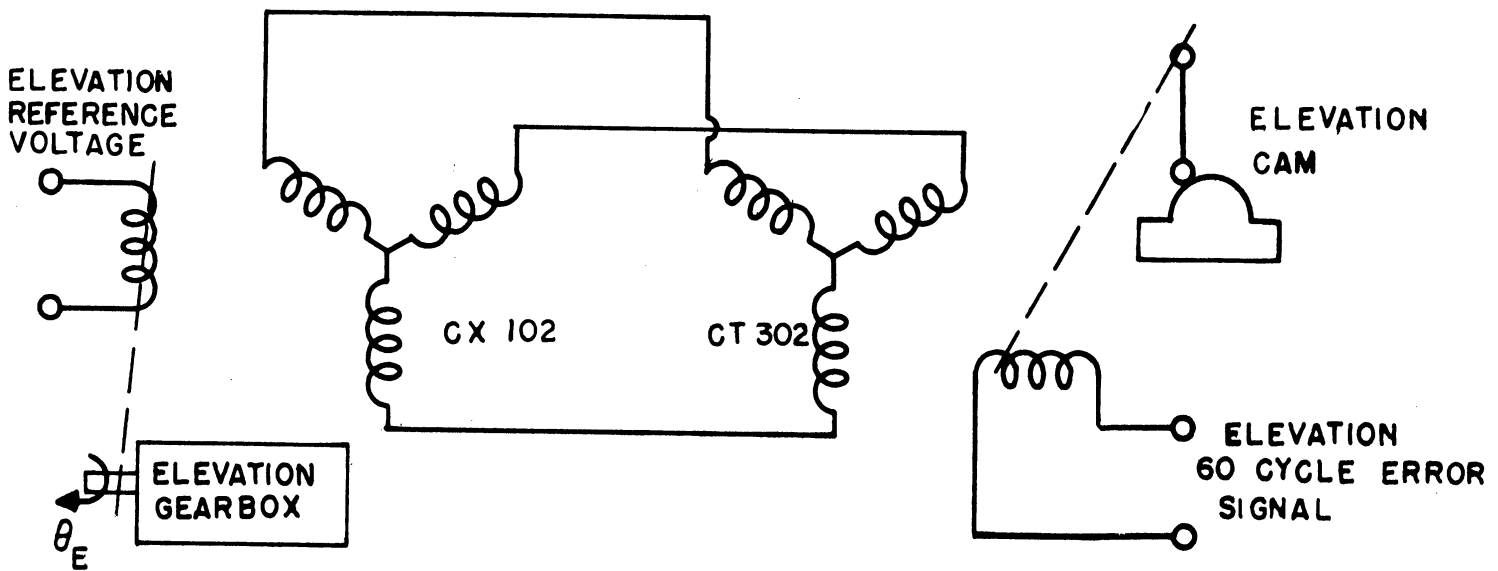
Figure 8   Elevation CX and CT Circuit

ELEVATION
GEARBOX

AZIMUTH
REFERENCE
VOLTAGE

θ_E

COSINE
TRANSFORMER
(CT 103)

CX 101

CT 301

AZIMUTH CAM

AZIMUTH
GEARBOX

θ_A

AZIMUTH 60 CYCLE
ERROR SIGNAL

Figure 9   Azimuth CX and CT Circuit
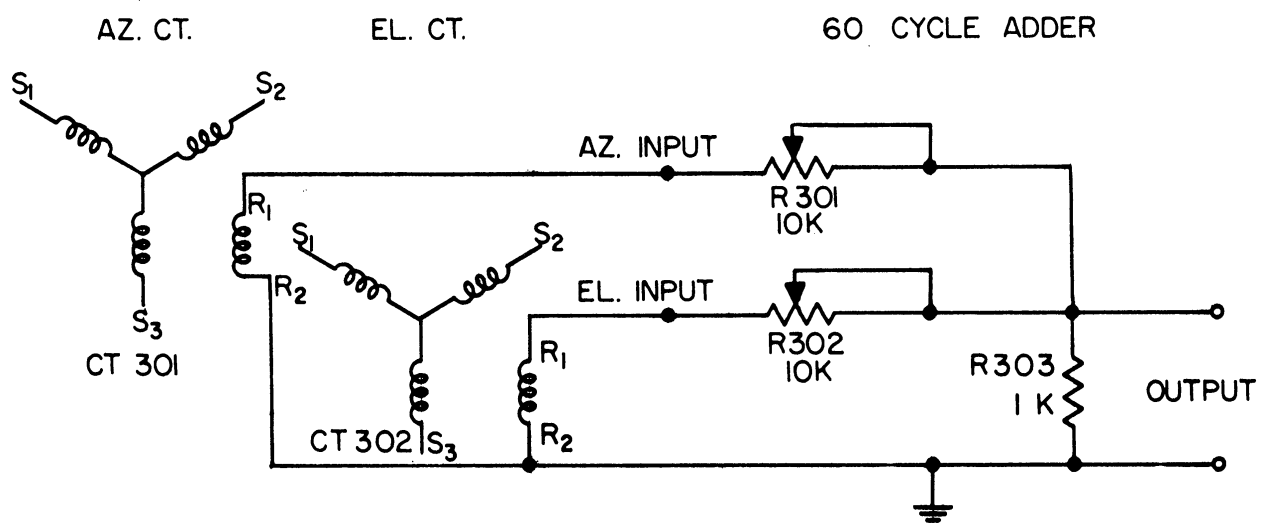
Figure 10   Sixty Cycle Adder Circuit

(a)
PHOTOTUBE
RESPONSE

(b)
SECTION OF
BEAM SHAPE
SIMULATOR
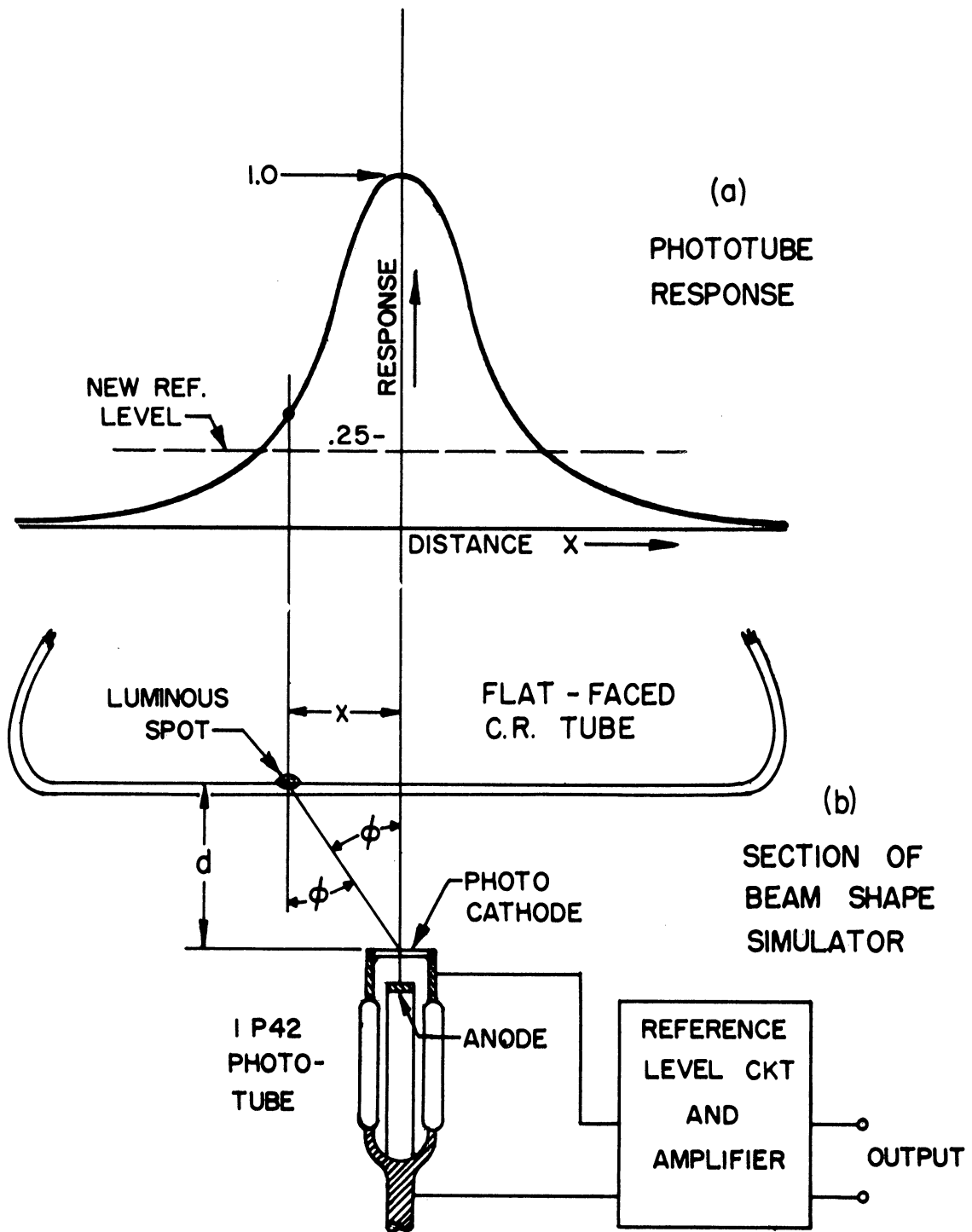
Figure 11   Principle of Beam Shape Generator
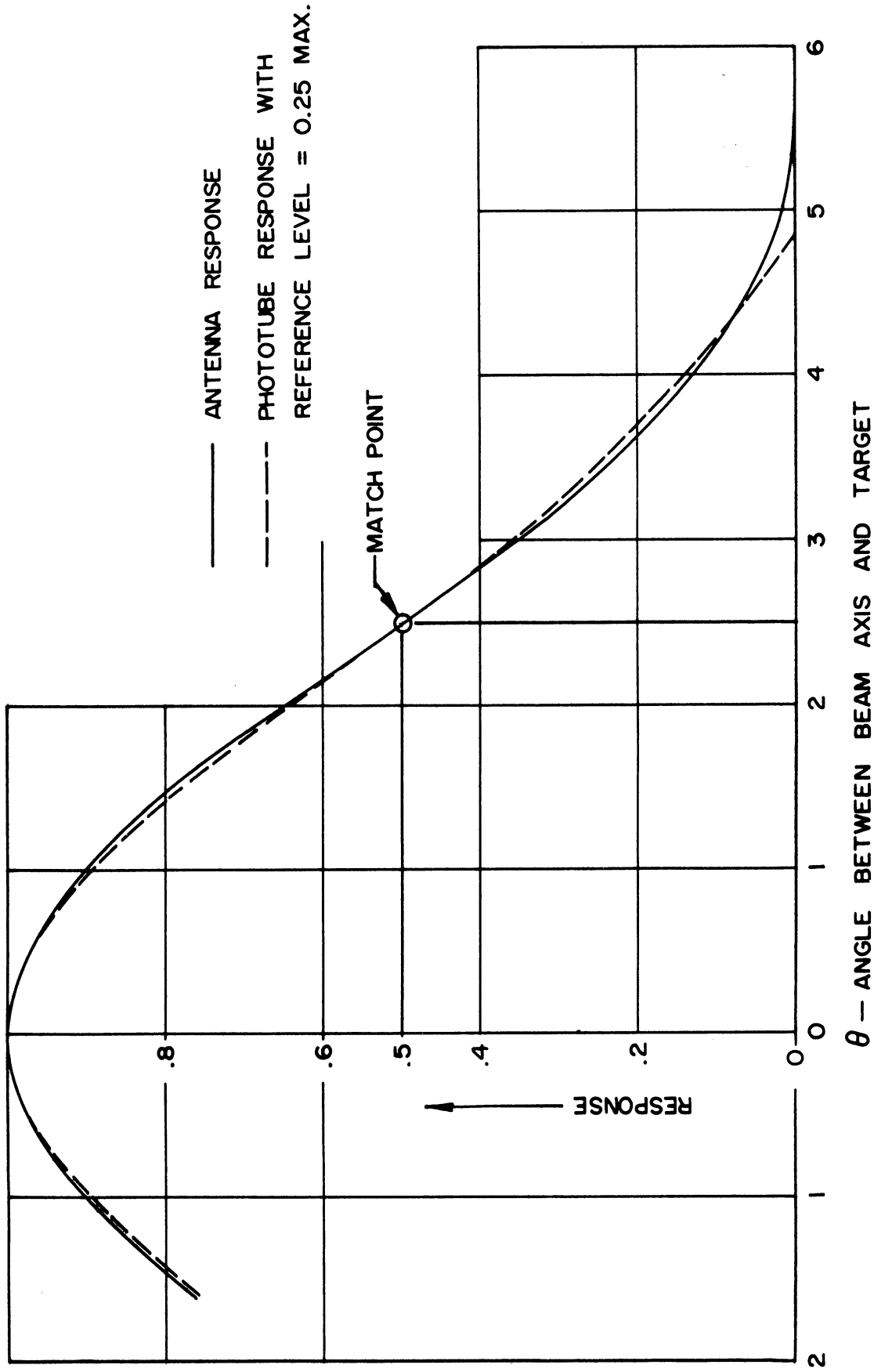
Figure 12   Theoretical Match Possible with Beam Generator
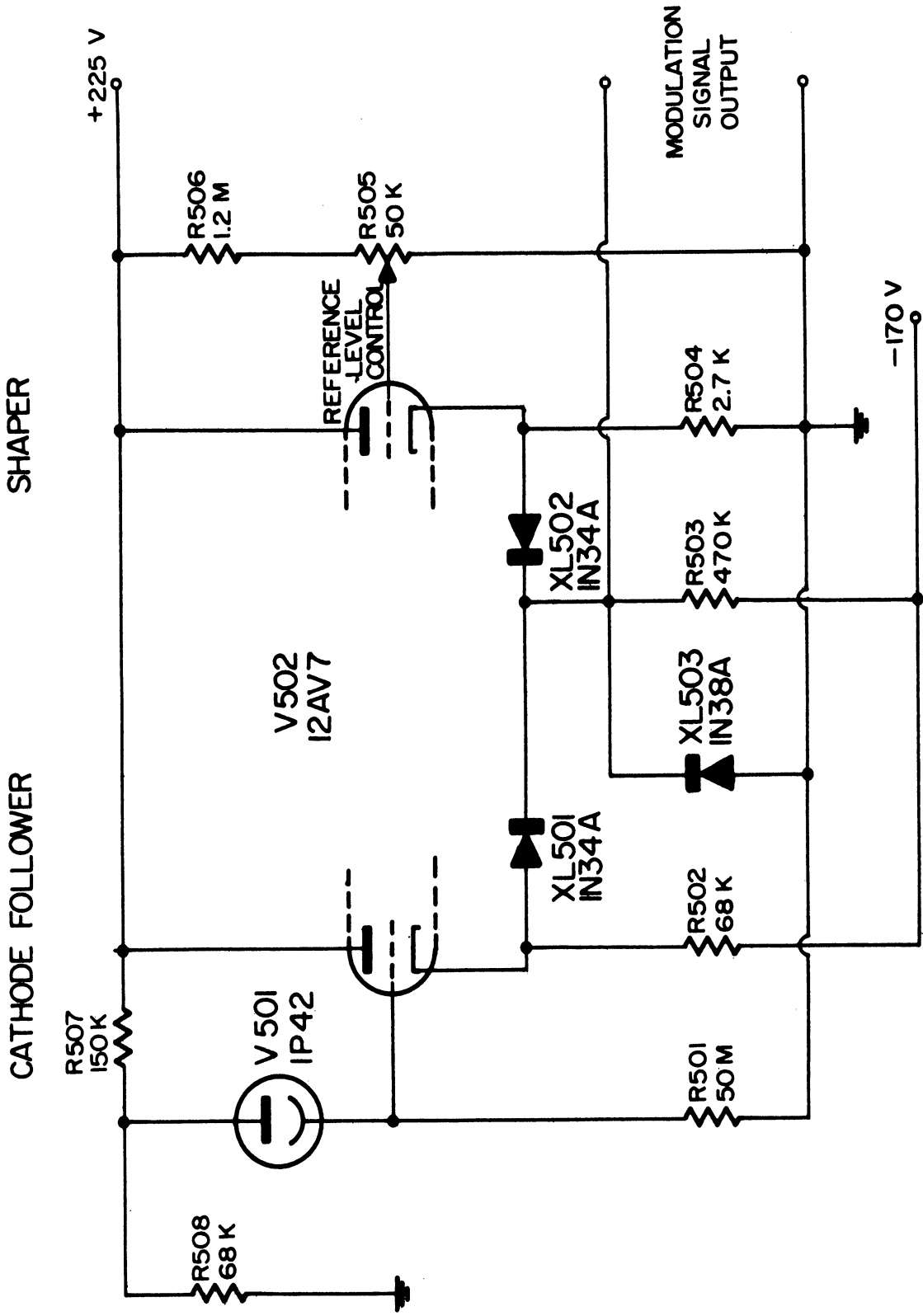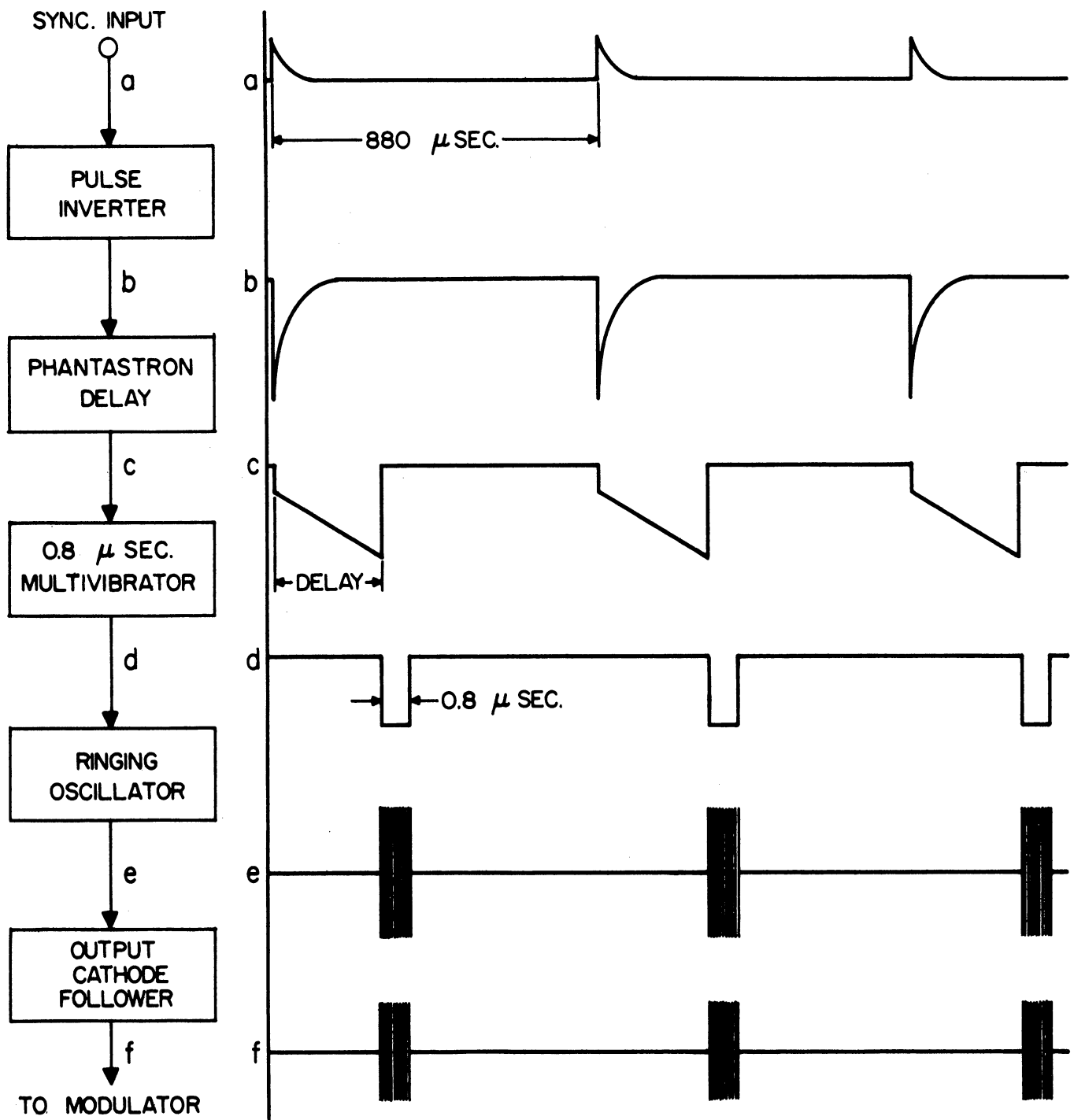
Figure 13 Cathode Follower and Shaper Circuit

SYNC. INPUT

a

PULSE
INVERTER

b

PHANTASTRON
DELAY

c

0.8 μ SEC.
MULTIVIBRATOR

d

RINGING
OSCILLATOR

e

OUTPUT
CATHODE
FOLLOWER

f

TO MODULATOR

a ├──── 880 μ SEC. ────┤

b

c ├─DELAY─┤

d →├← 0.8 μ SEC.

e

f

Figure 14 Block Diagram of Waveshapes of Pulse Generator and Oscillator
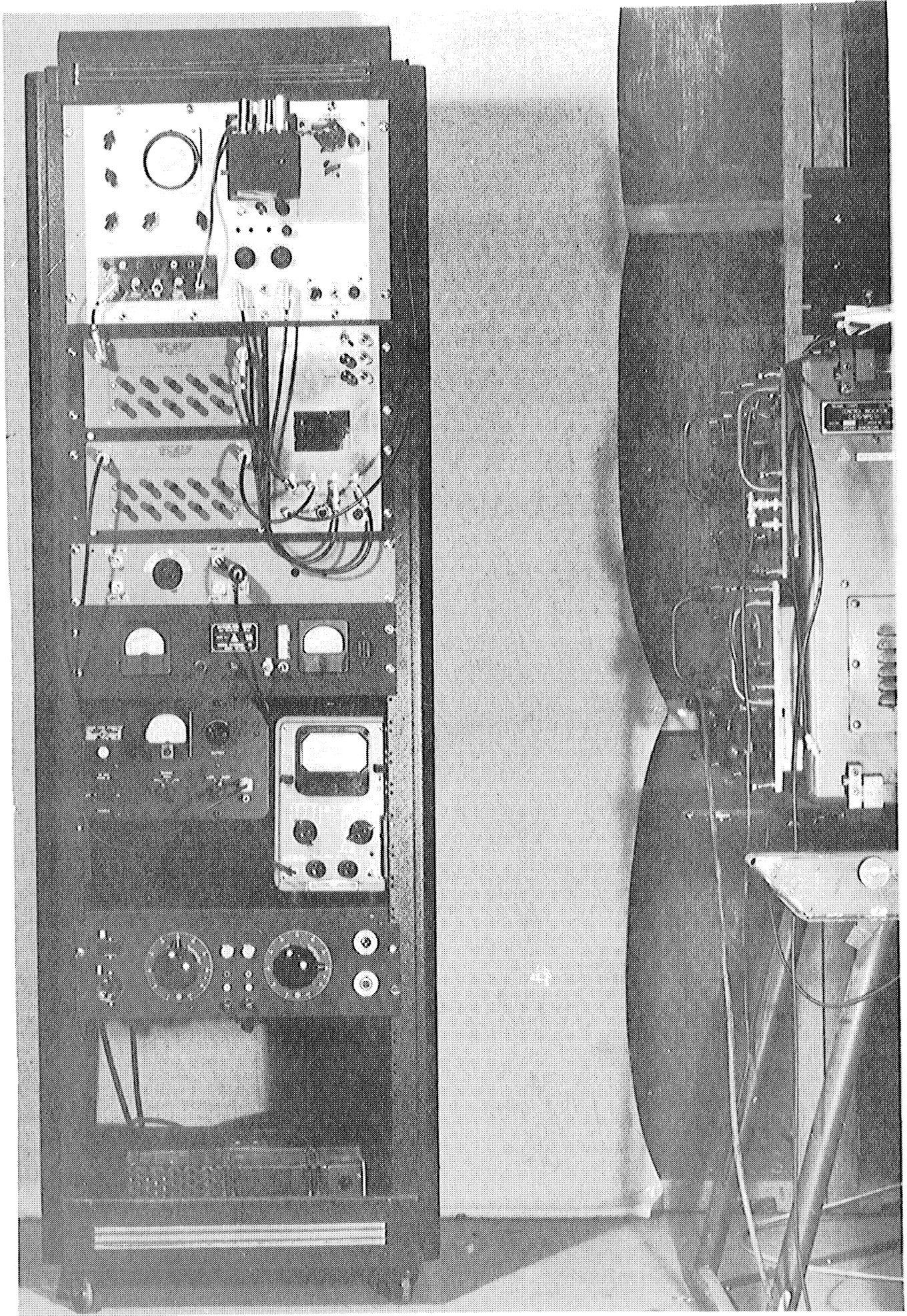
Figure 15   Photograph of Conical Scan Radar Target Simulator